DIAPHRAGM BEHAVIOR OF DECONSTRUCTABLE COMPOSITE FLOOR SYSTEMS

Lizhong Wang*, Mark D. Webster and Jerome F. Hajjar***

* Department of Civil and Environmental Engineering, Northeastern University, Boston, MA, USA
e-mails: wang.l@husky.neu.edu, jf.hajjar@neu.edu

** Simpson Gumpertz & Heger Inc., Waltham, MA, USA
e-mail: mdwebster@sgh.com

Keywords: Diaphragm behavior, Design for Deconstruction, Composite floor systems.

Abstract. *This study investigates the seismic behavior of deconstructable composite steel/concrete floor systems consisting of precast concrete planks and deconstructable clamping connections attaching the planks to the steel floor beams. The system is proposed to promote sustainable design of composite steel/concrete floor systems in steel buildings via reuse of the structural steel and concrete components at the end of the useful life of buildings. Finite element models representing a full-scale diaphragm were developed and analyzed. The load-displacement curves under cyclic loading present ductile diaphragm behavior of the proposed system under seismic loading. This behavior could be attributed to the observed limit states that include relative movement between adjacent planks and slip of the clamps that connect the steel girder and the girder plank, both of which occur after the frictional resistance is overcome.*

1 INTRODUCTION

Composite steel/concrete floor systems remain the most ubiquitous type of structural steel framing for commercial and residential buildings. Composite construction makes efficient use of the two materials, resulting in considerable increase of the flexural strength and stiffness of the steel beams. Accordingly, composite design provides a cost-effective solution by reducing the weight of the steel members and increasing the beam span. However, the integration of steel beams and concrete slabs via shear studs inhibits separation of the two materials, making impossible deconstruction of the conventional composite flooring systems and reuse of the structural components.

The building sector consumed almost half of the total energy used in U.S. in 2012, and was also responsible for 45% of all CO2 emission, far exceeding the transportation and industry sector[1]. In addition to the depletion of non-renewable resources and aggravating climate change, waste related to building construction and demolition is of concern. Construction and demolition (C&D) waste totals nearly 160 million tons per year, including debris generated during demolition (48 percent), renovation (44 percent) and new construction (8 percent)[2]. Design for Deconstruction of buildings aims at resolving these issues by reclaiming and repurposing the materials at the end of the service life of buildings.

As part of the floor and roof systems, diaphragms resist gravity and in-plane forces due to lateral loading. Under seismic loading, diaphragms are responsible for transferring the inertia forces within the floor systems to the seismic force-resisting systems. In addition, supports are provided by diaphragms to the vertical elements to prevent buckling and reduce the additional forces associated with P-delta effects[3]. For modelling and design, diaphragms are usually simplified as deep beams consisting of the following components: diaphragm slab; tension and compression chords, collectors, and the connections to the seismic force-resisting system. The strength and stiffness of a diaphragm can significantly affect

the seismic response of a building. Therefore, reasonable design and modelling assumptions used for diaphragms are fundamental to ensure structural integrity and desired performance during earthquakes.

This paper presents a new deconstructable composite floor system, comprising of precast concrete planks and steel beams connected using deconstructable clamping connectors, to promote sustainable design of composite floor systems in steel buildings and enable reuse of the structural components. The research program includes development of a prototype structure, analysis of the system and components for all relevant loadings, an experimental testing program that includes push-out tests of the clamping system, composite beam tests, and a series of tests of diaphragms subjected to in-plane loading. Finite element models are developed to investigate the failure modes and establish the behavior of the floor diaphragms. This paper presents preliminary results of this ongoing research, including analyses of the structural system subjected to cyclic loading as would be seen in earthquakes.

2 DECONSTRUCTABLE COMPOSITE FLOOR SYSTEM

The deconstructable composite beam prototype is illustrated in Figure 1. Precast concrete planks are firmly clamped to the steel beams, and frictional forces are thus generated at the steel/concrete interface, which could be utilized to achieve composite action in the floor system. Cast-in channels are embedded in the concrete planks to provide flexibility for where the beam intersects the planks and to allow for different beam width. Tongue and groove side joints in Figure 1 ensure that adjacent planks share loading, and offer a level and well-matched floor surface. By untightening the bolts, the clamping connectors enable the precast concrete planks and the steel beams to be easily disassembled and reconfigured in future projects.

Mechanical connectors are usually used in conventional precast concrete construction to transfer in-plane diaphragm forces. In order to achieve deconstructability of the system, grouting the planks and placing a cast-in place concrete topping, which help to tie all the planks together, are eliminated. Alternatively, the precast concrete planks are connected using unbonded threaded rods before being attached to the steel beams, as shown in Figure 2, with a pattern of connections aligned at 4’ on center and the planks staggered to help facilitate transfer of forces across the diaphragm. Friction, developed by pretensioning the rods, provides the resistance against joint sliding due to diaphragm shear and joint opening due to diaphragm flexure.

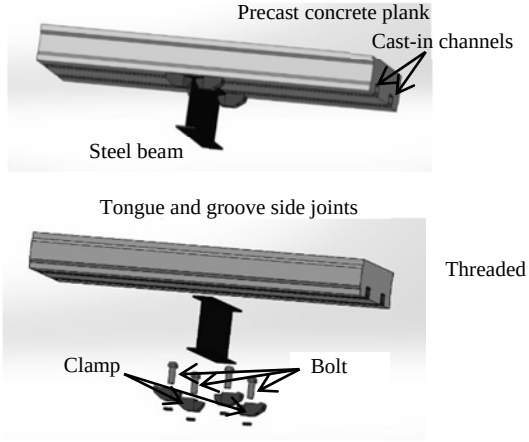

Figure 1. Deconstructable composite beam prototype

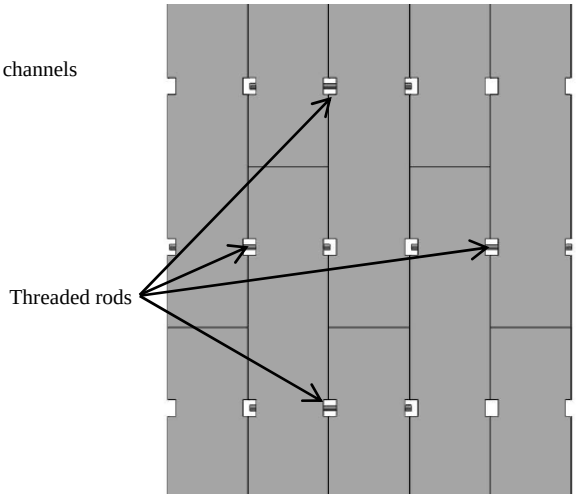

Figure 2. Precast concrete plank connections

Preliminary dimensions of the plank are 20 ft. x 2 ft. x 6 in, see Figure 3. This size is believed to be large enough to ensure structural integrity and reduce labor for construction and deconstruction but small enough to facilitate handling, transportation and reuse in new structures. Ideally, the planks are stocked in different sizes and concrete strengths for ready use, comparable to how steel is currently stocked at supply centers. A typical plan layout for a prototype office building using this system with a staggered plank configuration, as seen in Figure 2, is shown in Figure 4.

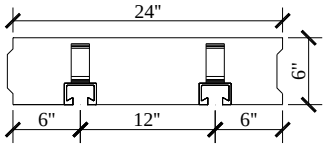

a) Plank perpendicular to steel beam

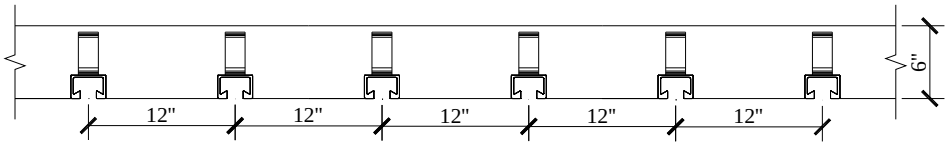

b) Plank parallel to steel girder

Figure 3. Precast concrete plank cross section (units: inches)

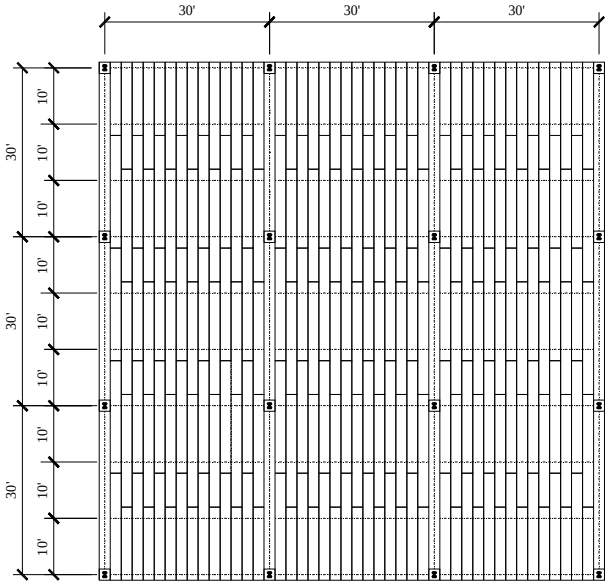

Notes:

1. The dashed lines show the steel framing. The beams are perpendicular to the precast concrete planks, while the girders are parallel to the planks.

2. Other precast plank patterns are also possible for the DfD system.

Figure 4. Typical floor plan for deconstructable composite floor system (units: feet)

3 FINITE ELEMENT ANALYSIS

This section presents nonlinear finite element analysis of this structural system to characterize its behavior. All the finite element models are developed in Abaqus/CAE and analyzed in Abaqus/Explicit. The analyses presented here employed the explicit method to solve quasi-static problems by applying cyclic loads sufficiently slowly to render the dynamic response negligible[4].

3.1 Finite element model and mesh

The finite element model, illustrated in Figure 5, represents half of a 30 ft. by 30 ft. diaphragm, which is composed of staggered precast concrete planks that are compressed together using threaded rods and then clamped to the steel beams. A similar test setup was utilized by Easterling and Porter[5] to investigate composite diaphragms. Steel beams with size W14x30 and W12x19, acting as the chords in the diaphragm, are selected to represent potential beam sizes in a gravity system, and the shear connectors are designed accordingly. W18x40 member is chosen as the steel girder that is part of the seismic force-resisting system along the perimeter. The number of connectors between the steel girder and the girder plank is varied to explore failure of the connection to the lateral force-resisting system. No reinforcement is used in the planks in these simulations.

Cast-in channels, as seen in Figure 1, are meshed with both eight-node reduced integration brick elements (C3D8R) and six-node reduced integration triangular prism elements (C3D6R), while the steel beams and concrete planks are meshed with C3D8R only. The complex geometry of the clamps and the bolts, modelled in detail in this work, necessitates use of four-node tetrahedron elements (C3D4).

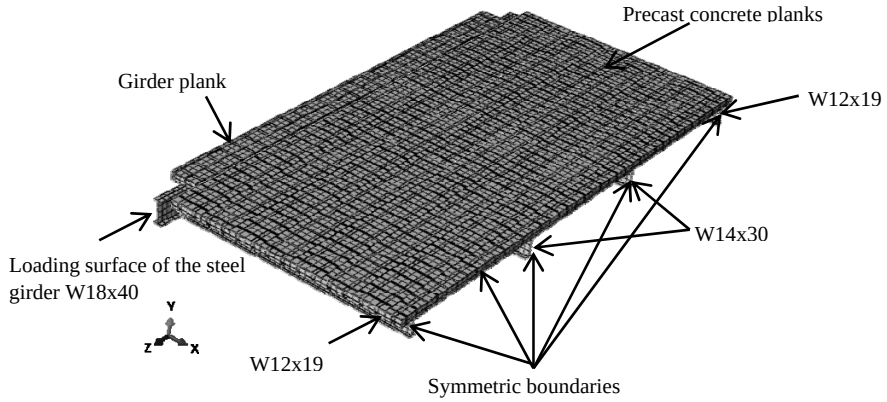

Figure 5. Finite element model for the diaphragm

3.2 Boundary conditions, load applications and contact

A symmetric boundary condition, as show in Figure 5, is defined such that nodes on these surfaces are prevented from translating in the X direction and rotating in the Y and Z directions. The ends of the steel girder are restrained from moving vertically to avoid rigid body motion of the system.

The loading history in these analyses is divided into three steps. Compression between planks is simulated by applying pressure on all the side surfaces of the diaphragm slab except for the surface where the boundary condition is defined, which is acceptable unless the response in the vicinity of the rods is studied. Bolt pretension is then obtained by assigning a thermal expansion coefficient and temperature change to the bolts, creating thermal shrinkage and generating tensile forces in the shank because of the constraints at the bolt ends. The steel girder is then subjected to cyclic loading using displacement control in the Z direction. The displacement history is provided in Figure 6. All the loadings are applied slowly and smoothly to minimize the dynamic effects and obtain a quasit-static solution. An optimal cyclic loading rate is found to be 0.125 mm/s.

The contact behavior between surfaces is defined in the normal direction and the tangential direction. “Hard contact”, the default normal behavior in Abaqus, puts no limit on the magnitude of the contact pressure when the contact restraint is activated once the surface clearance is zero. The contact restraint is removed when the surfaces separate, and the contact pressure becomes zero or negative. A penalty formulation, which allows a small amount of relative movement when the two surfaces are bonded, is used to characterize the behavior along the interface, and the frictional coefficient is taken as 0.3 for all the surfaces. General contact, rather than the contact pair algorithm, is selected to automatically define potential contact surfaces.

3.3 Material model

3.3.1 Material model for concrete

Concrete tensile cracking and compressive crushing are accounted for using the concrete damaged plasticity model provided in Abaqus. The tensile stress-strain relationship is linear elastic until the cracking stress is reached, and a softening stress-strain curve follows representing the formation of cracking. The compressive stress-strain response is linear elastic until the initial yield stress. The subsequent response is characterized by strain hardening and strain softening beyond the ultimate stress. Under cyclic loading, this concrete model can capture opening and closing of cracks observed in tests by allowing for stiffness recovery when the load is reversed.

Because mesh sensitivity exists for concrete with little or no reinforcement, tension stiffening is defined in terms of a stress-displacement curve rather than stress-strain curve to eliminate localization issues. The compressive stress-strain curve in BS EN 1992-1-1[6], provided in equation (1), is employed for this analysis. The elastic modulus can be calculated using equation (2). The Poission’s ratio is taken as 0.2.

$$\frac{\sigma_c}{f_{cm}} = \frac{k\eta - \eta^2}{1+(k-2)\eta} \tag{1}$$

$$E_{cm} = 22\left[\frac{f_{cm}}{10}\right]^{0.33} \tag{2}$$

Where,

f_{cm} = Mean value of concrete cylinder compressive strength (MPa)

σ_c = Concrete compressive stress (MPa)

$\eta = \dfrac{\varepsilon_c}{\varepsilon_{c1}}$

ε_c = Concrete compressive strain

ε_{c1} = Concrete compressive strain corresponding to peak stress f_{cm}

$\varepsilon_{c1} = 0.7 f_{cm}^{0.31} \le 2.8$

$k = \dfrac{1.05E_{cm} \times \varepsilon_{c1}}{f_{cm}}$

The default parameters specified in Abaqus for the concrete damaged plasticity model are used to characterize the plastic behavior under a general stress and strain state. The parameters include: dilation angle = 38° , eccentricity = 0.1. K_C , the ratio of the second invariant of the stress deviator on the tensile meridian to that on the compressive meridian at initial yield at a given first invariant of stress such that the maximum principal stress is negative, is equal to 0.67. The ratio of biaxial compressive yield stress to uniaxial compressive yield stress $\sigma_{b0} / \sigma_{c0}$ is taken as 1.16.

Concrete damage variables characterize stiffness degradation when the specimen is unloaded from any point on the softening branch. The damage variables range from zero for an undamaged model to one, exhibiting complete loss of strength and stiffness. Concrete tensile damage D_t and compressive damage D_c are derived using the following expressions:

$$D_t = 1 - \sigma_t / f_t \tag{3}$$

$$D_c = 1 - \sigma_c / f_c \tag{4}$$

3.3.2 Material model for steel members, cast-in channels and bolts

Elastic-perfectly-plastic material with a nominal yield stress of 345 MPa is defined for the steel beams and cast-in channels. The elastic modulus is taken as 200 GPa. The mechanical behavior is assumed to be the same in both tension and compression. A typical stress-strain curve for Grade 8.8 bolt material provided in Kulak et al. [7] is used for the analysis, as depicted in Figure 7.

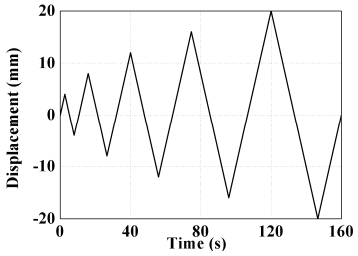

Figure 6. Loading history

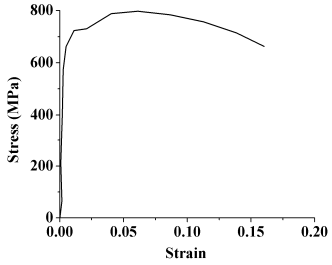

Figure 7. Bolt material stress-strain curve

3.4 Analysis results

The parameters for the analytical models are listed in Table 1, including the compressive stress between adjacent planks and the number of shear connectors between the steel girder and the girder plank. Different compressive stresses correspond to different spacing between the threaded rods. For example, when the threaded rods are placed at a distance of 4 ft., an equivalent compressive stress of 1.5 MPa is assumed. Although the steel girder is designed as a bare steel section, at least twenty shear connectors are needed to ensure a minimum of 25% composite action[8]. The spacing of the clamps is reduced from 3 ft. to 2 ft. when 28 clamps are used for the steel girder.

Table 1. Analytical model parameters

Model Number	Compressive stress (MPa)	Number of shear connectors
1	1.5	28
2	1.5	20
3	3.0	28
4	3.0	20
5	6.0	28
6	6.0	20

The cyclic load-displacement curves are plotted in Figure 8. The limit state for the first four models is joint sliding due to diaphragm shear; therefore, the compression between adjacent planks is directly related to the ultimate strength. The hysteresis loops are almost identical for Model 1 and Model 2, even though the number of shear connectors varies. A similar conclusion, however, cannot be reached for Model 3 and Model 4. The stiffness of Model 4 is smaller than that of Model 3, because the failure mode

for Model 4 is a combination of joint sliding and clamp slipping. Distinct load-displacement curves are plotted for Model 5 and Model 6, as their limit state is slip of the clamps between the steel girder and the girder plank. The number of shear connectors affects the ultimate strength of the diaphragms. All the diaphragms demonstrate ductile behavior with no strength and stiffness degradation.

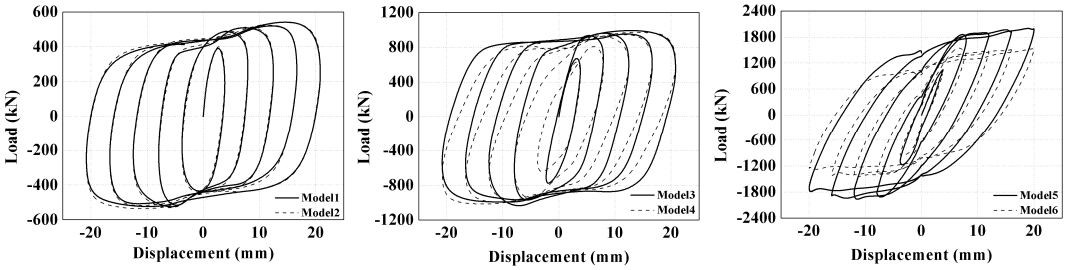

Figure 8. Cyclic load- displacement curves

In the diaphragm models, the moment at the symmetric boundaries is shared by the steel chords and the concrete slab in accordance with their relative stiffness. Figure 9 shows the ratio of the moment distributed to steel to the moment resisted by concrete for Model 1 during the cyclic loading process. Although the data points display some scatter, most range from 0.1 to 0.3. It can be concluded that the majority of the external force follows the stiffer load path and flows into the concrete slab, and the rest goes through the steel chords that are bent about their weak axis. This conclusion also applies to the other models, but the average ratio varies between 0.092 and 0.227.

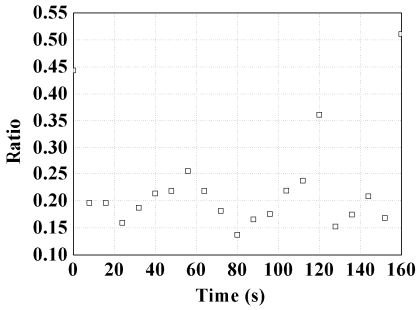

Figure 9. Steel moment to concrete moment ratio

While diagonal cracking may be seen in monolithic concrete diaphragms, this failure mode is uncommon in precast concrete diaphragms, since the joint between the diaphragms provides a weak link in the system. This argument is validated by minimal concrete tensile damage observed in the diaphragm models. Joint opening due to diaphragm bending, another potential limit state for a precast concrete diaphragm, did not occur for the models developed in this paper.

4 CONCLUSION

A new deconstructable composite floor system, which includes precast concrete planks and deconstructable clamping connections, was presented. The proposed system has the potential not only to maintain benefits offer by composite construction but also to enable disassembly and reuse of the structural components, thus closing the material flow loop and reducing energy consumption and material waste in the construction industry.

The diaphragm behavior of the new floor system was analyzed using six three-dimensional continuum models in which material nonlinearity and complex contact issues are accounted for. The following conclusions were obtained from the analysis results:

(1) Joint sliding is the limit state for models with a compressive stress between the planks of 1.5 MPa and 3.0 MPa (representing relatively light connections between the planks), and the diaphragm ultimate strength is strongly correlated to the magnitude of the normal stress.
(2) For models with a compressive stress between planks of 6.0 MPa, slip of the clamps governs. The number of shear connectors affects the ultimate strength of the diaphragms.
(3) Both limit states occur when the frictional resistance is overcome; therefore, ductile behavior is anticipated due to cyclic loading.
(4) The applied force to the steel girder is mainly distributed to the stiffer concrete slab. The ratio of the moment distributed to the steel chords to the moment distributed to the concrete slab typically varies between 0.092 and 0.227.
(5) Although no reinforcement is used in the planks, concrete remains intact except for localized damage near the clamps, since joint opening and sliding happen prior to the onset of concrete cracking due to in-plane bending and shear.

ACKNOWLEDMENTS

This material is based upon work supported by the National Science Foundation under Grant No. CMMI-1200820, the American Institute of Steel Construction, Northeastern University, and Simpson Gumpertz & Heger. Any opinions, findings, and conclusions expressed in this material are those of the authors and do not necessarily reflect the views of the National Science Foundation or other sponsors.

REFERENCES

[1] U.S. Energy Information Administration. *Annual Energy Review*. 2012.

[2] U.S.Environmental Protection Agency. *Municipal Solid Waste in the United States: 2007 Facts and Figures*. EPA 530-R-08-010. November 2008.

[3] Moehle, J. P., Hooper, J. D., Kelly, D. J., & Meyer, T. R. "Seismic Design of Cast-in-Place Concrete Diaphragms, Chords, and Collectors." *Seismic Design Technical Brief, US Department of Commerce, Building and Fire Research Laboratory, National Institute of Standards and Technology* 2010.

[4] Dassault Systèmes, *Abaqus 6.12 Theory Manual*. Dassault Systèmes Simulia Corp., Providence, Rhode Island, 2012.

[5] Easterling, W. S., & Porter, M. L. "Steel-Deck-Reinforced Concrete Diaphragms. I." *Journal of Structural Engineering, 120*, 560-576, 1994.

[6] EN, BS. 1-1: 2004 *Eurocode 2: Design of Concrete Structures. General Rules and Rules for Buildings*, 1992.

[7] Kulak, G. L., Fisher, J. W. and Struik, J. H. *Guide to Design Criteria for Bolted and Riveted Joints.* Vol. 2. New York: Wiley, 1987.

[8] AISC. Specification for Structural Steel Buildings (AISC 360-10), *American Institute of Steel Construction, Chicago, IL*, 2010.